JOURNAL OF AIRCRAFT
Vol. 46, No. 1, January–February 2009

Commercial Aircraft Exterior Cleaning Optimization

Mark Longmuir* and N. A. Ahmed†
University of New South Wales, Sydney, New South Wales 2052, Australia

DOI: 10.2514/1.38472

The time interval between aircraft exterior cleaning has traditionally been based upon experience and maintenance patterns rather than scientific reasoning. Therefore, the relationship between skin friction drag, aircraft exterior cleaning intervals, and fuel consumption has never been fully established or understood by airline operators. This work represents an attempt to investigate the effects of subtle changes in surface roughness on skin friction drag. Experiments were set up using several differently roughened surfaces. The results were analyzed and compared to a smooth reference surface which showed a clear correlation between skin friction drag with surface roughness. Surface roughness was reduced by approximately one-third as a result of aircraft washing in measurements taken from a sample of commercial aircraft. Using regression analysis of the surface measurements and relationships established in the experimentation, an optimum time interval between aircraft exterior cleaning was found. The optimum time frames recommended weighed the effects of the aerodynamic deterioration, due to surface roughness, against the costs involved in cleaning an aircraft. As a result a time interval between aircraft cleaning that maintains aerodynamic efficiency and cost practicality was achieved.

Nomenclature

AR	=	aspect ratio
a	=	speed of sound
C_D	=	drag coefficient
$C_{D,0}$	=	zero-lift parasite drag coefficient
C_f	=	skin friction drag coefficient
C_L	=	lift coefficient
c_T	=	thrust specific fuel consumption
D	=	drag force
E	=	lift-to-drag ratio
K	=	lift dependent drag factor
L	=	lift force
M	=	Mach number
N	=	Newton
R	=	range
Re	=	Reynolds number
R_a	=	average roughness height
R_{ti}	=	maximum roughness peak-to-valley distance in one cutoff length
R_{tm}	=	mean of R_{ti} in one assessment length, often referred to as R_z
R_y	=	maximum roughness peak-to-valley distance in one assessment length
R_z	=	refer to R_{tm}
S	=	plan form area
U	=	measured velocity
U_e	=	edge velocity
V	=	velocity
W_f	=	fuel weight
W_0	=	initial weight
W_1	=	final weight
δ	=	boundary-layer thickness
δ_x	=	displacement thickness
θ_x	=	momentum thickness

Received 13 May 2008; revision received 15 October 2008; accepted for publication 16 October 2008.

*Currently Production Engineer, Qantas Engineering, Qantas Jet Base S-AB1/10, Qantas Drive, Mascot, NSW, 2020, Australia.

†Associate Professor, School of Mechanical and Manufacturing Engineering.

Introduction

AIRLINES throughout the world clean the exterior of an aircraft with the aim of maintaining visual appearance, corrosion protection, and to reduce fuel burn. Many airline operators assume that a regularly cleaned aircraft is an aircraft that suffers from less skin friction drag and consequently less fuel burn.

Traditionally the time interval between aircraft exterior cleaning has been based upon experience and maintenance patterns rather than scientific reasoning. Therefore, the relationship between skin friction drag, aircraft cleaning intervals, and fuel consumption has never been fully established or understood by airline operators.

This work represents an attempt to investigate the effects of subtle changes in surface roughness on skin friction drag. By expressing increases in drag in terms of fuel burn an optimum time interval between aircraft cleaning was determined.

The majority of the data generated for the behavior of fluid flow over roughened surfaces originates from the paper by Nikuradse [1]. Nikuradse's experiments lead to a large amount of drag data for sand grain roughness with a depth of projection between 0.01 and 0.16 cm. Because of its simplicity, Nikuradse's experiment has been used to explain the behavior of generic and naturally occurring surfaces, although, the surfaces used by Nikuradse do not physically relate to rough surfaces occurring in nature [2].

Grigson [3] asserts that experimental testing of surfaces allows accurate determination of a roughness function. Numerous studies on locally applied roughness to lifting surfaces are well reported, particularly leading edges. However, there is a scarceness of data documenting the effects of subtle changes in roughness on aerodynamic performance.

Only recently have studies been conducted on a roughness scale that has not been previously reported. Many of the later papers carry out experiments using abrasive paper roughness as a base, due to the known roughness qualities, to determine the skin friction at a smaller scale.

Abdel-Rahman and Chakroun [4] conducted an investigation of the effects of abrasive paper roughness on lift at Reynolds numbers between 1.7×10^5 and 3.4×10^5, indicating a trend that $C_{D,0}$ increases with an increased scale of roughness. The roughness also increased C_L by delaying drag separation in the stall region. However, roughness decreased the maximum lift-to-drag ratio by as much as 55% depending on the grade of the roughness.

Schultz [2] documented the differences in frictional resistance of an unsanded to polished surfaces of a flat plate. Schultz found that the frictional resistance increased up to 7.3% for an unsanded, as-sprayed surface compared to a polished surface.

There is a wide variety of roughness heights that can increase drag being recommended by aircraft manufacturers and researchers. Some of the roughness heights suggested to cause increased drag are 28 μm [5], 300 μm [6], and 5 μm [7], creating some confusion on the impact of surface roughness.

Boeing [8] has suggested, for their class of aircraft, that surface roughness only makes up 0.4% of the total aircraft drag. Nevertheless, estimates of increased fuel burn due to roughened areas on aircraft range from 310 U.S. gallons per year for a 0.93 m^2 area [9] to 500 U.S. gallons per year for a 1 m^2 area [6]. Hence, the extra fuel burn can represent a substantial cost to an airline with a large fleet.

Many variables have to be considered when adopting an approach for aircraft cleaning. The blanket assumption of a smooth aircraft being an efficient aircraft is difficult to sustain. Variables such as a faster deterioration of the paint by cleaning, associated labor costs, and the minimal benefits due to drag reduction have to be considered. A cost benefit analysis assists in providing a practical relationship between the costs in cleaning an aircraft to the benefits gained by drag reduction. Even though the benefits gained by small changes in surface roughness are minimal, by following the "drop in the bucket" theory, there is still room for gains while maintaining a vigil on operational efficiency and cost.

The aim of this paper and the experiments conducted were to study the effects of surface roughness on skin friction drag and boundary-layer behavior. The skin friction drag was measured by wind-tunnel testing for a variety of roughened surfaces. In conjunction to the wind-tunnel testing, measurements of the boundary layer, displacement and momentum thickness for different kinds of abrasive paper were completed. These experiments assisted in establishing a relationship between an increase in surface roughness and drag. By using this relationship a cost analysis was carried out to determine the optimum time interval to clean an aircraft.

Experimental Apparatus

Of the several wind tunnels available for a multitude of research work [10–17] and located in the Aerodynamics Laboratory of the University of New South Wales, two subsonic wind tunnels with different features were considered more appropriate and were used in the experiments.

A closed circuit wind tunnel with force balance measurement facilities was used to investigate drag variations due to different surface roughness. This closed circuit wind tunnel had a 1.2 m high, 0.9 m wide test section with an airspeed range of 0–45 m/s.

An open circuit boundary-layer wind tunnel was used to measure the velocity profiles of the airflow adjacent to differently roughened surfaces. This tunnel, however, did not have the arrangements to measure drag directly. The open circuit boundary-layer tunnel had a test section 0.21 m high and 0.56 m wide with a contraction ratio of inlet-to-test-section height of 5. The maximum speed of the open circuit tunnel was 25 m/s.

Instrumentation

The closed circuit wind tunnel had a six-axis external force balance (load cell) located beneath the test section transmitting aerodynamic forces and moments via three supports. The load cell was demonstrated to have a sensitivity of 0.1 N. A pitot-static tube, connected to a digital manometer, measured the real time flow velocity within the test section.

The open circuit boundary-layer experiment used a five-hole probe to measure the velocity profile of the flow adjacent to the roughened surfaces. The five holes allowed the measurement [18–20] of the airflow's three-dimensional characteristics. The calibration of the probe was conducted in a manner as described in detail by Pissasale and Ahmed [21] for low flow angularity as would be expected on a conventional wing surface. The five tubes of the probe were connected to the input ports of a pressure transducer which in turn was connected to a computer using a Labview program to record the pressure readings.

Table 1 Painted panel roughness measurements

Panel roughness	R_a, μm	$R_{y\max}$, μm	R_z, μm	% change $R_{y\max}$
Plain painted panel	0.2	2.2	1.8	0%
Scotchbrite	0.375	3.8	3.13	73%
1000 grit roughened	0.43	5.25	3.76	139%
600 grit roughened	0.65	5.3	4.75	141%
180 grit roughened	1.17	10.37	8.27	371%
60 grit roughened	1.39	14.77	11.11	571%

Model Configuration

Several $300 \times 235 \times 2.032$ mm (0.080 in.) thick 2024-T3 clad aluminum flat plate panels were manufactured and painted to represent the fuselage exterior finish of a Boeing 747. The panels were painted with a urethane compatible primer, Boeing Material Specification (BMS) 10 type III and PPG Industries civil aviation product CA8000 white BAC70846 (BMS 10–60 type II polyurethane enamel) top coat. Both the primer and top coats were applied as per the Boeing Aircraft Maintenance Manual [22].

Six panels were manufactured in total and each panel was roughened by a different grade of abrasive paper. The different abrasive papers used were a 1000, 600, 180, and 60 grit. Another panel was roughened with a Scotchbrite scrub and a final panel was left smooth so as to be used as a reference point for the experimental testing. Care was taken to ensure the entire panel was evenly sanded by hand to achieve a uniform roughness.

A surface analyzer (Surfanalyser 5000) was used to measure the surface roughness of the test panels. Data were taken from a cutoff length of 0.80 mm with five cutoff lengths per traverse length. Four samples were taken at random positions on each panel and averaged to give the final surface roughness value. The roughness parameters of the test panels are given in Table 1.

The painted panels used in the closed circuit wind-tunnel experiment offered small variations in surface roughness. Because of the maximum open circuit boundary-layer tunnel speed of 25 m/s, the small variation in roughness was not pronounced enough to determine any differences in the velocity profile at such low speeds. To enhance differences in velocity profiles, different grades of abrasive paper were used as an illustration of the effects of surface roughness on drag. Three different grades of standard 228.6×279.4 mm (9×11 in.) abrasive paper (60, 180, and 1000) and one smooth panel were used.

Experimental Procedure

Closed Circuit Wind-Tunnel Experiment

The experiments were completed at Reynolds numbers varying between 8.9×10^5 and 9.16×10^5. Each roughened panel was mounted to the three vertical supports connected to the load cell and set at a zero angle of attack by the use of a digital spirit level. Ten measurements were taken to ensure reliability and reduce uncertainty of the results as only small changes in the drag values were expected. Drag measurements were taken at 15, 30, and 45 m/s. After each run the test piece was removed and replaced with a different roughened panel and the experiment repeated.

Open Circuit Wind-Tunnel Experiment

The boundary-layer experiments took place over Reynolds numbers varying between 4.98×10^5 and 5.14×10^5. The abrasive papers and smooth panel were adhered to a steel dividing plate within the tunnel by the use of double-sided tape and experimentation took place at the maximum tunnel velocity of 25 m/s.

A five-hole probe was lowered to the center of the test section and a measurement of the undisturbed freestream airflow was taken. The probe was lowered until it was adjacent to the test piece and pressure measurements recorded. The probe was then raised 0.5 mm and another set of measurements taken. The measurement process was completed in progressive increments until the velocity of the airflow reached 99% of the value of the freestream air indicating the edge of

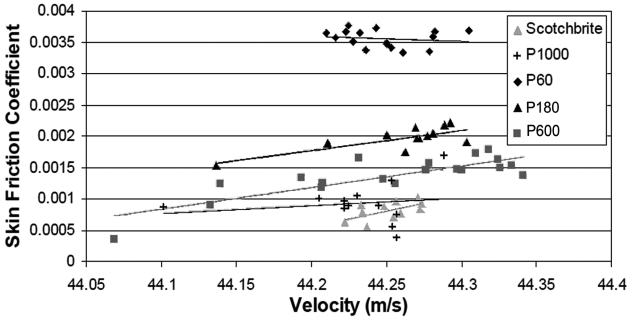

Fig. 1 Painted panel skin friction coefficient results.

the boundary layer [23]. Measurements of the velocity profile were taken 95, 190, and 270 mm along the length of each test piece.

Experimental Results and Discussion

Aerodynamic Drag Results

Figure 1 illustrates the skin friction drag coefficient results of the differently roughened painted panels measured in the closed circuit wind tunnel. The results show a clear distinction in coefficient values between the different roughened surfaces. Some overlapping of the scatter does occur especially between the smoother surfaces; however, overlapping was expected due to the small scale of variations in roughness heights between the smoother surfaces.

An averaged percentage increase in skin friction drag using the smooth surface as a reference was calculated and is summarized in Table 2. Using a least-squares fit, an equation relating a percentage increase in roughness to a percentage increase in skin friction drag was derived. This is given by Eq. (1):

$$\%\ \text{drag increase} = 1 \times 10^{-6}\ (\%\ \text{roughness increase})^2 + 0.0086\ (\%\ \text{roughness increase}) + 0.4228 \quad (1)$$

Because of the small variation in surface roughness of operational aircraft an exact replication of the surface roughness heights could not be achieved in this experiment. Equation (1) is expressed in terms of a percentage rather than actual skin friction coefficient values. Using percentages allowed the results to be related to an aircraft rather than the flat painted panels of the experiment.

Boundary-Layer Results

Using the open circuit wind tunnel the boundary-layer profiles at various positions were investigated as shown in Fig. 2. Figure 3 shows a comparison of the boundary-layer results taken 270 mm along the test piece length against the theoretical power laws [23].

It was found that the roughest surface (60 grit) velocity profile was impeded to a greater extent than the other surfaces at all positions. As the surface became smoother, the amount of retardation of the flow reduced. This difference in velocity profiles is indicative of boundary-layer thickness increases. It took a height of 12 mm for the velocity adjacent to a the 60 grit surface to return to 99% of the freestream airflow compared to 7 mm for the smooth panel at the 270 mm position. A comparison against the theoretical power laws, Fig. 3, shows a trend of the rougher surfaces following the higher turbulent theoretical approximation. The velocity profile of the 60 grit surface aligned closer with the one-ninth power law while the

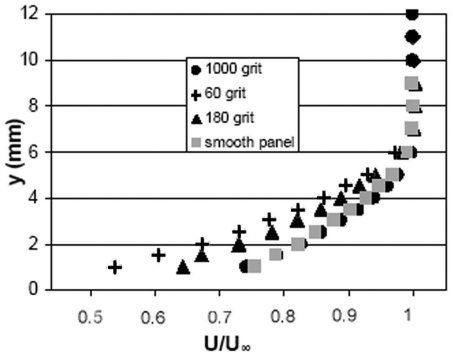

a) 90 mm position

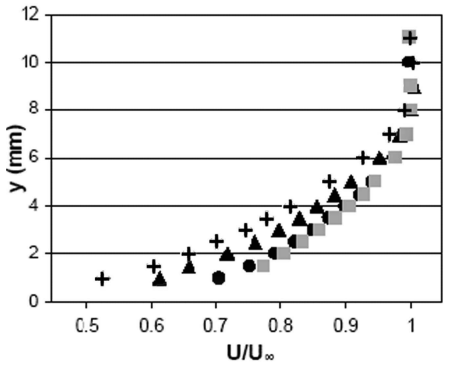

b) 190 mm position

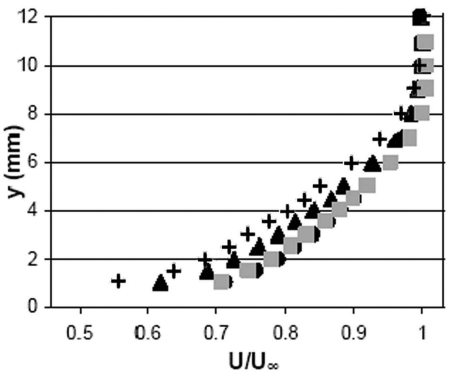

c) 270 mm position

Fig. 2 Velocity profiles at various positions.

smooth panel and 1000 grit surface closely followed the one-fifth power law indicating that the degree of turbulence experienced by the flow was increased for a rougher surface.

The boundary layer also grew from 8 to 12 mm along the length of the 60 grit abrasive paper. This boundary-layer growth was due to the fluid being decelerated further by increased viscous stresses. A similar result is achieved for the displacement thickness and momentum thickness shown in Tables 3 and 4.

When comparing the Reynolds number of the experiment to a commercial aircraft at cruise conditions of 45×10^6 [24], simulation errors could occur. However, theoretically the boundary-layer

Table 2 Painted panel drag results summary table

Roughness parameter	Thickness, mm	Average velocity, m/s	Average percentage increase in skin friction, μm	R_y, μm	Percentage increase in R_y
60	2.032	44.26	5.9%	14.8	571%
150	2.032	44.26	3.23%	10.7	371%
600	2.032	44.25	2.24%	5.3	141%
1000	2.032	44.23	1.52%	5.2	139%
Scotchbrite	2.032	44.25	1.34%	3.8	73%
Painted	2.032	44.24	——	2.2	——

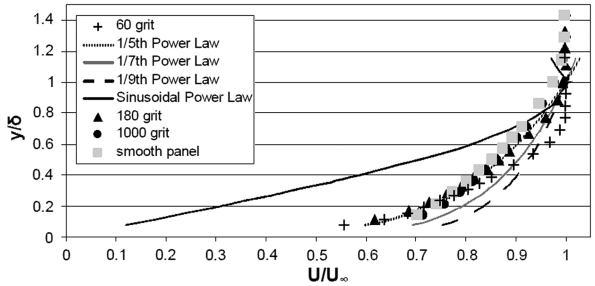

Fig. 3 Comparison of experimental velocity profiles to theory at the 270 mm position.

thickness is proportional to $Re^{-1/5}$ for turbulent flow. A surface can be considered aerodynamically smooth if the roughness elements are less than the viscous sublayer thickness because the roughness elements do not protrude into the airflow. As the Reynolds number increases the boundary layer decreases and the surface can change from being aerodynamically smooth to rough due to the roughness elements protruding into the viscous layer. It can therefore be theoretically suggested that the impact of surface roughness on drag, developed via the wind-tunnel experiments, may be amplified due to the boundary layer reducing and more roughness elements protruding into the freestream at a higher Reynolds number.

Skin Friction Coefficient

The skin friction coefficient can be calculated from the momentum integral relation (Karman integral relation) given by Eq. (2) [25]:

$$\frac{C_f}{2} = \frac{\mathrm{d}\theta}{\mathrm{d}x} + (2+H)\frac{\theta}{U_e}\frac{\mathrm{d}U_e}{\mathrm{d}x} \tag{2}$$

The boundary-layer experiments were carried out on flat test pieces where the edge velocity U_e of the boundary layer remained relatively constant. Therefore, the derivative of the edge velocity $\mathrm{d}U_e/\mathrm{d}x$ is approximately equal to zero and Eq. (2) is equal to a derivative of the momentum thickness equation:

$$\frac{C_f}{2} \approx \frac{\mathrm{d}\theta}{\mathrm{d}x} \tag{3}$$

Table 5 compares experimental and theoretical calculation of the boundary-layer skin friction coefficients. Theoretical calculations are a function of the Reynolds number as given by Anderson [26] for laminar flow and Schlichting and Gersten [23] for turbulent flow.

Table 5 shows a clear distinction between the different grades of roughness with a higher skin friction coefficient for a rougher surface. It is interesting to note that as the surface roughness increases, the experimental skin friction coefficient value moves away from the theoretical laminar coefficient to the theoretical turbulent coefficient value suggesting an increase in the level of turbulence. It must be noted that the variation in the experimental C_f values can be attributed to the differences in the Reynolds number in the experiment and the abrasive paper used in the open circuit boundary-layer wind-tunnel experiment for explanatory purposes.

Overall, the results of the skin friction coefficient measurements proved that a higher degree of roughness creates a higher skin friction coefficient value. Therefore, the conclusion that a significant increase in C_f due to surface roughness compared to a smooth surface can be made.

Cost/Benefit Analysis

To develop an optimum time interval to clean an aircraft that is aerodynamic and cost effective three relationships had to be established:

1) A percentage increase in friction drag due to a percentage increase in surface roughness.

2) An increase in surface roughness to a time interval between aircraft cleaning.

3) An increase in fuel burn due to an increase in skin friction drag.

The relationship between skin friction drag and surface roughness was found in the initial experiments given by Eq. (1). The other two relationships were found by the measurement of the surface roughness of a large sample of commercial aircraft and the manipulation of a theoretical range equation. Because these

Table 3 Experimental displacement thickness along the abrasive paper length

Position mm	Smooth plate displacement thickness, δ_x mm	1000 grit displacement thickness, δ_x mm	180 grit displacement thickness, δ_x mm	60 grit displacement thickness, δ_x mm
95	0.86	0.83	1.19	1.57
190	0.98	1.06	1.38	1.80
270	1.08	1.12	1.52	1.97

Table 4 Experimental momentum thickness along the abrasive paper length

Position mm	Smooth plate momentum thickness, θ_x mm	1000 grit momentum thickness, θ_x mm	180 grit momentum thickness, θ_x mm	60 grit momentum thickness, θ_x mm
95	0.63	0.60	0.75	0.92
190	0.73	0.75	0.88	1.09
270	0.77	0.84	1.03	1.27

Table 5 Skin friction coefficient comparison

Surface roughness	Painted panel wind-tunnel experiment, C_f	Boundary-layer experiment, C_f	Laminar theoretical, C_f	Turbulent theoretical, C_f
Smooth	——	0.0016	0.00098	0.00545
1000 grit	0.00093	0.0028	——	——
180 grit	0.00210	0.0032	——	——
60 grit	0.00360	0.0040	——	——

relationships are all linked, fuel burn can be expressed in terms of a time interval between cleaning.

Surface Roughness Measurement, Data Collection, and Analysis

Instrumentation

Surface roughness measurements of aircraft were completed using a Taylor–Hobson profilometer (Surtronic 3P model 112/1550) battery operated display-transverse unit and pickup. The profilometer used had an overall accuracy of 2% ±1 unit in the least significant figure. The unit contains a drive motor which traverses the pickup across the surface to be measured. The traverse length is selected by a switch that allows for three separate transverse lengths, 0.25, 0.8, and 2.5 mm. The pickup is a variable reluctance-type transducer with a diamond tip stylus with a tip radius of 5 μm. Surface roughness measurements were taken in accordance with ISO 4288:1996(E) [27] on a large sample of commercial aircraft at Sydney's Mascot Airport in February 2007.

Analysis

The profilometer used was limited to measuring only R_a, R_y, and R_{tm} roughness parameters. The R_y parameter is the maximum height from peak to valley in one assessment length and was chosen for analysis due to its greater sensitivity and variation within the data samples. Analysis was carried out on the forward and aft zones of an aircraft separately. The forward zone was considered any area of the aircraft forward of the wings leading edge and highly sensitive to changes in surface smoothness [6]. The forward zone had a mean R_y of 0.44 μm compared to the aft zone of 0.99 μm. By the use of a regression analysis a relationship between roughness height and the time intervals between aircraft cleaning was found as given in Table 6.

The poor relationship of the forward zone regression analysis was due to the inherent smooth nature of the forward zone; thereby, any changes in surface roughness over time were difficult to distinguish.

Comparison Before and After a Wash

A surface roughness measurement of a 737–800 before and after a wash was completed and is summarized in Table 7. It was found that the maximum roughness heights were reduced at all areas measured after a wash. This reduction was on the order of 30% of the R_y value.

Fuel Burn Cost and Skin Friction Drag Relationship

Several assumptions were required to establish fuel burn increases due to surface roughness. To approximate aircraft drag it is assumed that only 10% of an aircraft's surface area is affected by surface roughness as only the forward portion of the aircraft experiences uninterrupted flow. The forward zone surface roughness to time period relationship was used in all calculations. It was also assumed that skin friction drag increases affect parasite drag ($C_{D,0}$) only and not drag due to lift (KC_L^2) of an aircraft's total drag. Finally, the fuel burn costs were evaluated over the cruise section of an aircraft flight. It is assumed that the impact of surface roughness is small compared to other drag factors during takeoff and landing rotations.

To approximate fuel burn during cruise a range equation was used. When flight is conducted under the jurisdiction of air traffic control regulations, constant altitude/constant airspeed cruise flight is applied. For a jet aircraft the range equation is given by Eq. (4) [28]:

$$R = \frac{2VE_m}{c_T}\left(\tan^{-1}2\frac{\sqrt{k/C_{D_0}}W_0}{\rho V^2 S} - \tan^{-1}2\frac{\sqrt{k/C_{D_0}}W_1}{\rho V^2 S}\right) \quad (4)$$

Assuming that the lift-to-drag ratio is a maximum, then

$$E_m = \frac{1}{2(KC_{D_0})^{1/2}} \quad (5)$$

By rearranging Eq. (4) the landing weight W_1 of an aircraft can be determined by Eq. (6):

$$W_1 = \frac{\rho V^2 S}{2\sqrt{k/C_{D_0}}}\tan\left[\tan^{-1}\left(\frac{2\sqrt{k/C_{D_0}}W_0}{\rho V^2 S}\right) - \frac{c_T R}{2VE_m}\right] \quad (6)$$

Equation (1) gave a percentage increase in skin friction drag as a function of a percentage increase in surface roughness. By arbitrarily selecting a percentage increase in surface roughness and applying the resulting percentage increase in drag to an aircraft's $C_{D,0}$ value the landing weight can be determined. This is calculated by specifying the range R to fly and assuming all other aircraft parameters remain constant. Because the takeoff weight of an aircraft W_0 is known and the landing weight W_1 can be calculated by Eq. (6), the difference between the two is the fuel weight used in flight and is given by Eq. (7):

$$W_f = W_0 - W_1 \quad (7)$$

Fuel Burn and Skin Friction Drag

The aircraft parameters used in the range equation are summarized in Table 8. These parameters are estimates taken from Cavcar [29] and the base of aircraft data (BADA) aircraft performance summary tables [30].

The fuel specification and prices used are detailed in Table 9. These specifications are based on the 2007 fuel cost per barrel. With today's volatility of the fuel prices the impact of fuel is a major concern for all aircraft operators and gives weight to the necessity to improve fuel usage where possible.

Fuel Burn and Aircraft Cleaning Interval Relationship

Three related relationships have been established. From the sampled aircraft measurements the surface roughness height was given as a function of a time between cleaning. Through wind-tunnel experimentation, skin friction drag was expressed as a function of

Table 6 Regression analysis results of surface roughness and time between aircraft cleaning

Aircraft position	R^2	P value	Regression line
Fwd zone	1.2%	0.0016	$R_y = 0.5118 - 0.004042$ (days since wash) $+ 0.000048$ (days since wash)^2
Aft zone	25.4%	0.0028	$R_y = 0.301 + 0.04068$ (days since wash) $- 0.000228$ (days since wash)^2

Table 7 R_y data summary of aircraft washing

Variable	General position	No. of data points	Mean, R_y, μm	Median, R_y, μm	Standard deviation, R_y, μm	Min, R_y, μm	Max, R_y, μm
Before wash	Engine	4	0.85	0.90	0.45	0.34	1.27
	Flap upper surface	6	0.43	0.35	0.23	0.21	0.85
	Main landing gear (MLG) door	6	0.37	0.31	0.21	0.18	0.76
After wash	Engine	8	0.41	0.30	0.25	0.18	0.94
	Flap upper surface	6	0.25	0.29	0.14	0.00	0.38
	MLG door	6	0.38	0.35	0.14	0.22	0.61

Table 8 Aircraft parameters

Parameter	747–400	767–300	737–800	Units
Takeoff weight	362,880	158,000	79,015	kg
Wing area	524.9	283.3	125.0	m^2
Parasite drag coefficient	0.0268	0.014	0.020	——
Induced drag coefficient	0.043	0.049	0.055	——
Specific fuel consumption (sea level)	0.75	0.75	0.75	kg fuel/thrust/h
Cruise speed	0.85	0.75	0.75	Mach
Cruise altitude	9450	9450	9450	m
Relative air density	0.335	0.335	0.335	——
Relative fuel consumption @9450 m	0.00017	0.00017	0.00017	kg fuel/thrust/s
Density @9450 m	0.01528	0.01528	0.01528	kg/m^3
Temperature @9450 m	234.21	234.21	234.21	K
Velocity	260.8	240.9	240.9	m/s

Table 9 Jet-A specifications

Fuel density[a]	807.5	kg/m^3
Fuel cost per barrel[b]	86.3	U.S. $
Fuel cost per gallon	2.06	U.S. $
Weight of 1 U.S. gallon	3.057	kg
Foreign exchange rate[c]	0.8011	——
Fuel cost per kg	0.841	AUD

[a]Shell material safety data sheet version no. 1.1, 29 June 2005.
[b]Data available online at http://www.iata.org/whatwedo/economics/fuel_monitor/index.htm [retrieved Sept. 2007].
[c]Data available online at http://www.rba.gov.au/Statistics/exchange_rates.html [retrieved 27 July 2007].

surface roughness height. Finally, by the use of the range equation, fuel burn cost has been related changes in skin friction drag. Because all these relationships are connected cumulative fuel burn costs can be expressed in terms of a time interval between cleaning as plotted in Fig. 4.

To find the optimum time interval the fuel burn costs have to be compared to the costs to clean an aircraft as shown in Fig. 5. Selecting an arbitrary labor rate of the Australian dollar (AUD) 62.41 (U.S. $50) per labor hour a general approximation of the costs associated to clean the exterior of an aircraft can be estimated. It is assumed that the labor cost includes material costs and that no other costs are incurred due to aircraft downtime. The total cost to wash an aircraft is given in Table 10 [22].

Table 10 Labor power and cleaning cost

Aircraft	Aircraft wash labor requirements, h	Wash costs
737	3	$187.24
763	4	$249.66
747	6	$374.49

Using the reduction in surface roughness height by 30% after washing, the aircraft's optimum wash interval can be established for the life cycle of an aircraft as shown in Fig. 6.

Table 11 summarizes the intersection points of an aircraft's cleaning and fuel burn costs for different aircraft and ranges. The general trend in Table 11 shows a reduction in the time frame between cleaning for increased ranges flown. For a 1% variation in surface roughness reduction due to washing there is a corresponding change in the optimum time period to clean an aircraft varying between 0 and 5% depending on the aircraft type and the range flown.

The reduction in time frames was expected; however, a greater decrease was anticipated. The initial weak relationships established in the surface roughness statistical analysis could contribute to the

Table 11 Optimal cleaning time interval summary tables

Boeing 747 aircraft							
Range, km	2000	4000	6000	8000	10,000	12,000	14,000
Wash, days	44	44	43	42	41	40	39
Boeing 767 aircraft							
Range, km	2000	4000	6000	8000			
Wash, days	42	40	39	35			
Boeing 737 aircraft							
Range, km	1000	2000	3000	4000			
Wash, days	47	42	41	38			

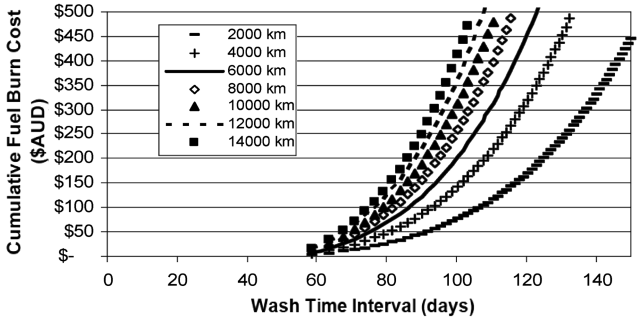

Fig. 4 747–400 cumulative fuel burn cost to wash interval for different ranges: forward zone.

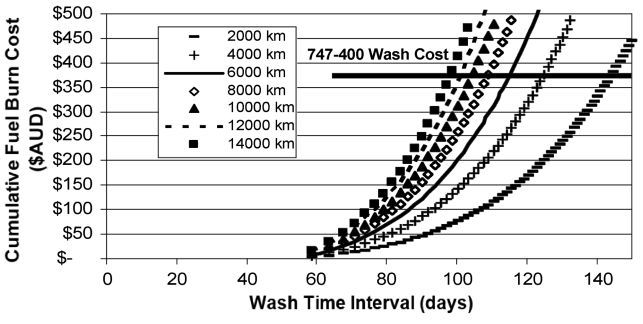

Fig. 5 Wash cost and fuel cost intersection for the 747–400: forward zone.

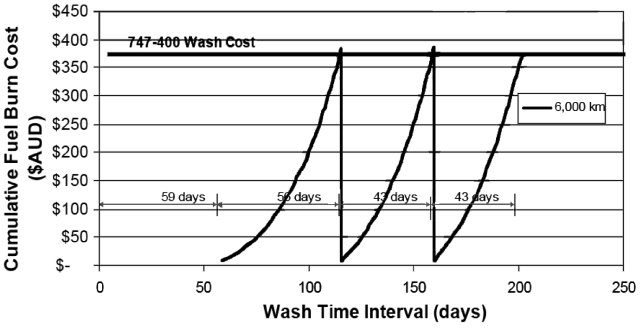

Fig. 6 Optimum wash interval for the 747–400 forward zone for 6000 km range.

gradual decrease. Time periods listed in Table 11 give the optimum time interval to clean an aircraft that is both aerodynamic and cost efficient.

Conclusions

The initial closed circuit wind-tunnel testing showed that for an increase in surface roughness there was a corresponding increase in the skin friction drag. Further investigation found that surface roughness promoted an increase in turbulence with a thickening of the boundary layer.

By carrying out a cost analysis of fuel burn and aircraft cleaning costs an optimum time interval to clean an aircraft was formulated. It was concluded that the appropriate time interval to wash an aircraft reduced as the distance flown by an aircraft increased.

Overall, experimental testing as well as statistical and theoretical analysis has been applied to a practical problem. It is anticipated that the time frames concluded for aircraft cleaning enable the effects of aerodynamic deterioration to be traded against the costs involved in cleaning an aircraft. In doing so a balance between aerodynamic efficiency and cost practicality has been achieved.

References

[1] Nikuradse, J., "Laws of Flow in Rough Pipes," National Advisory Committee for Aeronautics, TM 1292, translated 1950, 1933.

[2] Schultz, M. P., "The Relationship Between Frictional Resistance and Roughness for Surfaces Smoothed by Sanding," *Journal of Fluids Engineering*, Vol. 124, 2002, pp. 492–499. doi:10.1115/1.1459073

[3] Grigson, C. W. B., "Drag Losses of New Ships Caused by Hull Finish," *Journal of Ship Research*, Vol. 36, No. 2, 1992, pp. 182–196.

[4] Abdel-Rahman, A. A., and Chakroun, W. M., "Surface Roughness Effects on Flow Over Airfoils," *Wind Engineering*, Vol. 21, No. 3, 1997, pp. 125–137.

[5] Boeing Airlines Flight Operations Engineering "Boeing Fuel Conservation Newsletter," No. 41, Flight Technical Section, 1991.

[6] Airbus Flight Operations Support—Customer Services Directorate, "Getting Hands on Experience with Aerodynamic Deterioration—A Performance Audit View," STL 945.3399/96, No. 2, 2001.

[7] Miklosovic, D. S., and Schultz, M. P., "Effects of Surface Finish on Aerodynamic Performance of a Sailboat Centerboard," *Journal of Aircraft*. Vol. 41, No. 5, 2004, pp. 1073–1081. doi:10.2514/1.777

[8] Shure, C., "Drag Assessment—Performance Engineer Operations," Flight Operation Boeing Presentation, 1998.

[9] Boeing Commercial Airplane Company, "Airplane Maintenance for Fuel Conservation B767," Rept. D622T004, 1986.

[10] Simpson, R. G., Ahmed, N. A., and Archer, R. D., "Improvement of a Wing Performance Using Coanda Tip Jets," *Journal of Aircraft*, Vol. 37, No. 1, 2000, pp. 183–184. doi:10.2514/2.2579

[11] Simpson, R. G., Ahmed, N. A., and Archer, R. D., "Near Field Study of Vortex Attenuation Using Wing Tip Blowing," *The Aeronautical Journal*, Vol. 102, March 2002, pp. 117–120.

[12] Gatto, A., Ahmed, N. A., and Archer, R. D., "Investigation of the Upstream End Effect of the Flow Characteristics of a Yawed Circular Cylinder," *The Aeronautical Journal*, Vol. 104, No. 1033, March 2000, pp. 125–128.

[13] Gatto, A., Ahmed, N. A., and Archer, R. D., "Surface Roughness and Free Stream Turbulence Effects on the Surface Pressure Over a Yawed Circular Cylinder," *Journal of Aircraft*, Vol. 38, No. 9, Sept. 2000, pp. 1765–1767.

[14] Gatto, A., Byrne, K. P., Ahmed, N. A., and Archer, R. D., "Pressure Measurements Over a Cylinder in Crossflow Using Plastic Tubing," *Experiments in Fluids*, Vol. 30, No. 1, 2001, pp. 43–46. doi:10.1007/s003480000133

[15] Rashid, D. H., Ahmed, N. A., and Archer, R. D., "Study of Aerodynamic Forces on a Rotating Wind Driven Ventilator," *Wind Engineering*, Vol. 27, No. 1, 2003, pp. 63–72. doi:10.1260/030952403321833770

[16] Shun, S., and Ahmed, N. A., "Utilizing Wind and Solar Energy as Power Sources for a Hybrid Building Ventilation Device," *Renewable Energy*, Vol. 33, No. 6, June 2008, pp. 1392–1397. doi:10.1016/j.renene.2007.07.017

[17] Findanis, N., and Ahmed, N. A., "The Interaction of an Asymmetrical Localised Synthetic Jet on a Side Supported Sphere," *Journal of Fluids and Structures*, Vol. 24, No. 7, 2008 pp. 1006–1020. doi:10.1016/j.jfluidstructs.2008.02.002

[18] Pissasale, A., and Ahmed, N. A., "Theoretical Calibration of a Five Hole Probe for Highly Three Dimensional Flow," *Measurement Science and Technology*, Inst. of Physics Publishing, London, Vol. 13, 2002, pp. 1100–1107.

[19] Pissasale, A., and Ahmed, N. A., "Examining the Effect of Flow Reversal on Seven-Hole Probe Measurements," *AIAA Journal*, Vol. 41, No. 12, 2003, pp. 2460–2467. doi:10.2514/2.6845

[20] Pissasale, A., and Ahmed, N. A., "Development of a Functional Relationship Between Port Pressures and Flow Properties for the Calibration and Application of Multi-Hole Probes to Highly Three-Dimensional Flows," *Experiments in Fluids*, Vol. 36, No. 3, March 2004, pp. 422–436. doi:10.1007/s00348-003-0740-8

[21] Pissasale, A., and Ahmed, N. A., "A Novel Method of Extending the Calibration Range of Five Hole Probe for Highly Three Dimensional Flows," *Flow Measurement and Instrumentation*, Elsevier, New York, Vol. 13, Nos. 1–2, March–April 2002, pp. 23–30.

[22] Boeing 747-400 Aircraft Maintenance Manual, "Decorative Paint System—Cleaning and Painting," 51-24-11-701, 2007.

[23] Schlichting, H., and Gersten, K., *Boundary Layer Theory*, 8th ed., Springer, New York, 2003.

[24] Crook, A., "Skin Friction Estimation at High Reynolds Numbers and Reynolds Number Effects for Transport Aircraft.," *Center for Turbulence Research Annual Research Briefs*, 2002, pp. 427–436.

[25] Cebci, T., and Smith, A. M. O., *Analysis of Turbulent Boundary Layers*, Academic Press, New York, 1974.

[26] Anderson, J. D., *Fundamentals of Aerodynamics*, 3rd ed., McGraw–Hill, New York, 2001.

[27] International Standard, "Geometrical Product Specifications (GPS)—Surface Texture: Profile Method—Rules and Procedures for the Assessment of Surface Texture," ISO 4288:1996(E), 1996.

[28] Hale, F. J., *Introduction to Aircraft Performance, Selection and Design*, Wiley, New York, 1984.

[29] Cavcar, A., and Cavcar, M., "Impact of Aircraft Performance Characteristics on Air Traffic Delays," *Turkish Journal of Engineering and Environmental Sciences*, Vol. 28, No. 1, 2004, pp. 13–23.

[30] Eurocontrol, "Aircraft Performance Summary Tables for the Base of Aircraft Data (BADA)," EEC Note No. 18/00, Rev. 3.3, 2000.